An Eigensystem Realization Algorithm
for Modal Parameter Identification and Model Reduction

Jer-Nan Juang* and Richard S. Pappa*
NASA Langley Research Center, Hampton, Virginia

A method called the eigensystem realization algorithm is developed for modal parameter identification and model reduction of dynamic systems from test data. A new approach is introduced in conjunction with the singular-value decomposition technique to derive the basic formulation of minimum order realization which is an extended version of the Ho-Kalman algorithm. The basic formulation is then transformed into modal space for modal parameter identification. Two accuracy indicators are developed to quantitatively identify the system and noise modes. For illustration of the algorithm, an example is shown using experimental data from the Galileo spacecraft.

Introduction

THE state space model has received considerable attention for system analyses and design in recent control and systems research programs. One of these areas, in particular, is control of large space structures. In order to design controls for a dynamic system it is necessary to have a mathematical model that will adequately describe the system's motion. The process of constructing a state space representation from experimental data is called system realization.

During the past two decades, numerous algorithms for the construction of state space representations of linear systems have appeared in the controls literature. Among the first were the works of Gilbert[1] and Kalman,[2] introducing the important principles of realization theory in terms of the concepts of controllability and observability. Both techniques use the transfer function matrix to solve the realization problem. Ho and Kalman[3] approached this problem from a new viewpoint. They showed that the minimum realization problem is equivalent to a representation problem involving a sequence of real matrices known as Markov parameters (pulse response functions). By minimum realization is meant a model with the smallest state space dimension among systems realized that has the same input-output relations within a specified degree of accuracy. Questions regarding the minimum realization from various types of input-output data and the generation of a minimum partial realization are studied by Tether,[4] Silverman,[5] and Rossen and Lapidus[6] using Markov parameters. Rossen and Lapidus[7] successfully applied Ho-Kalman[3] and Tether[4] methods to chemical engineering systems. A common weakness of the preceding schemes is that effects of noise on the data analysis were not evaluated. Zeiger and McEwen[8] proposed a combination of the Ho-Kalman algorithm[3] with the singular-value decomposition technique for the treatment of noisy data. However, no theoretical or numerical studies were reported by Zeiger and McEwen. Among follow-up developments along similar lines, Kung[9] presented another algorithm in conjunction with the singular-value decomposition technique to incorporate the presence of the noise. Note that the singular-value decomposition technique[10,11] has been widely recognized as being very effective and numerically stable. Although several techniques of minimum realization are available in the literature, formal direct application to

modal parameter identification for flexible structures has not been addressed.

In the structures field, the finite element technique is used almost exclusively for constructing analytical models. This approach is well established and normally provides a model accurate enough for structural design purposes. Once the structure is built, static and dynamic tests are performed. These test results are used to refine the finite element model, which is then used for final analyses. This traditional approach to analytical model development may not be accurate enough for use in designing a vibration control system for flexible structures. Another approach is to realize a model directly from the experimental results. This requires the construction of a minimum-order model from the test data that characterizes the dynamics of the system at the selected control and measurement positions. The present state-of-the-art in structural modal testing and data analysis is one of controversy about the best technique to use. Classical test techniques, which may provide only good frequency and moderate mode shape accuracy, are often considered adequate for finite element model verification purposes. On the other hand, advanced data analysis techniques that offer significant reductions in test time and improved accuracy have been available,[12-16] but are not yet fully accepted. For example, Vold and Russell[16] presented a method using frequency-response functions and time-domain analysis for direct identification of modal parameters including repeated eigenvalues. A comparison of contemporary methods using data from the Galileo spacecraft test is provided by Chen.[17]

Although structural dynamics techniques are generally successful for ground data, further incorporation with work from the controls discipline is needed to solve modal parameter identification/control problems. For example, it is known from control theory[18] that a system with repeated eigenvalues and independent mode shapes is not identifiable by single input and single output. Methods which allow only one initial condition (input) at a time[13] will miss repeated eigenvalues. Also, if the realized system is not of minimum order and matrix inversion is used for constructing an oversized state matrix, numerical errors may become dominant.

Under the interaction of structure and control disciplines, the objective of this paper is to introduce an eigensystem realization algorithm (ERA) for modal parameter identification and model reduction for dynamical systems from test data. The algorithm consists of two major parts, namely, basic formulation of the minimum-order realization and modal parameter identification. In the section of the basic formulation, the Hankel matrix, which represents the data structure for the Ho-Kalman algorithm, is generalized to allow ran-

dom distribution of Markov parameters generated by free decay responses. A unique approach based on this generalized Hankel matrix is developed to extend the Ho-Kalman algorithm in combination with the singular-value decomposition technique.[10,11] Through the use of the generalized Hankel matrix, a linear model is realized for a dynamical system matching the input and output relationship. The realized system model is then transformed into modal space for modal parameter identification. As part of ERA, two accuracy indicators, namely, the modal amplitude coherence and the modal phase collinearity, are developed to quantify the system and noise modes. The degree of modal excitation and observation is evaluated. The ERA method thus forms the basis for a rational choice of model size determined by the singular values and accuracy indicators.

Experimental results for a complex structure—the Galileo spacecraft—are given to illustrate the ERA method. The Galileo spacecraft is an interplanetary vehicle to be launched in 1986 for a detailed investigation of the planet Jupiter and its moons.

Basic Formulations

A finite dimensional, discrete-time, linear, time-invariant dynamical system has the state-variable equations

$$x(k+1) = Ax(k) + Bu(k) \tag{1}$$

$$y(k) = Cx(k) \tag{2}$$

where x is an n-dimensional state vector, u an m-dimensional control input, and y a p-dimensional output or measurement vector. The integer k is the sample indicator. The transition matrix A characterizes the dynamics of the system. For flexible structures, it is a representation of mass, stiffness, and damping properties. The problem of system realization is as follows: Given the measurement functions $y(k)$, construct constant matrices $[A, B, C]$ such that the functions y are reproduced by the state-variable equations. Any system has an infinite number of realizations that will predict the identical response for any particular input. Let T be any nonsingular square matrix. The triple $[TAT^{-1}, TB, CT^{-1}]$ will also be a realization.[6] However, the eigenvalues of the matrix A are preserved.

For the system Eqs. (1) and (2) with free pulse response, the time domain description is given by the function known as the Markov parameter

$$Y(k) = CA^{k-1}B \tag{3}$$

or in the case of initial state response

$$Y(k) = CA^k [x_1(0), x_2(0), \ldots, x_m(0)]$$

where $x_i(0)$ represents the ith set of initial conditions and k is an integer. Note that B is an $n \times m$ matrix and C is a $p \times n$ matrix. The problem of system realization is: Given the functions $Y(k)$, construct constant matrices $[A,B,C]$ in terms of $Y(k)$ such that the identities of Eq. (3) hold. The algorithm begins by forming the $r \times s$ block matrix (generalized Hankel matrix)

$$H_{rs}(k-1)$$

$$= \begin{bmatrix} Y(k) & Y(k+t_1) & \cdots & Y(k+t_{s-1}) \\ Y(j_1+k) & Y(j_1+k+t_1) & \cdots & Y(j_1+k+t_{s-1}) \\ \vdots & \vdots & & \vdots \\ Y(j_{r-1}+k) & Y(j_{r-1}+k+t_1) & \cdots & Y(j_{r-1}+k+t_{s-1}) \end{bmatrix} \tag{4}$$

where $j_i (i=1,\ldots,r-1)$ and $t_i (i=1,\ldots,s-1)$ are arbitrary integers. For the system with initial state response measurements, simply replace $H_{rs}(k-1)$ by $H_{rs}(k)$. Now observe that

$$H_{rs}(k) = V_r A^k W_s; \quad V_r = \begin{bmatrix} C \\ CA^{j_1} \\ \cdot \\ \cdot \\ CA^{j_{r-1}} \end{bmatrix}$$

and

$$W_s = [B, A^{t_1}B, \ldots, A^{t_{s-1}}B] \tag{5}$$

where V_r and W_s are the observability and controllability matrices, respectively. Note that V_r and W_s are rectangular matrices with dimensions $rp \times n$ and $n \times ms$, respectively. Assume that there exists a matrix $H^\#$ satisfying the relation

$$W_s H^\# V_r = I_n \tag{6}$$

where I_n is an identity matrix of order n. It will be shown that the matrix $H^\#$ plays a major role in deriving the ERA. What is $H^\#$? Observe that, from Eqs. (5) and (6),

$$H_{rs}(0)H^\# H_{rs}(0) = V_r W_s H^\# V_r W_s = V_r W_s = H_{rs}(0) \tag{7}$$

The matrix $H^\#$ is thus the pseudoinverse of the matrix $H_{rs}(0)$ in a general sense. For a single input, there exists a case [see Eq. (5)] where the rank of $H_{rs}(0)$ equals the column number of $H_{rs}(0)$, then

$$H^\# = [[H_{rs}(0)]^T H_{rs}(0)]^{-1} [H_{rs}(0)]^T \tag{8}$$

On the other hand, there exists a case for a single output [see Eq. (5)] where the rank equals the row number, then

$$H^\# = [H_{rs}(0)]^T [H_{rs}(0) [H_{rs}(0)]^T]^{-1} \tag{9}$$

The matrix $H_{rs}(1)H^\#$ has been used in the structural dynamics field to identify system modes and frequencies.[13] This is a special case representing a single input which cannot realize a system that has repeated eigenvalues, or a noise-free system unless the system order is known a priori. More discussion can be found in the Appendix.

A general solution for $H^\#$ is given below. For an nth-order system, find the nonsingular matrices P and Q such that [10,11]

$$H_{rs}(0) = PDQ^T \tag{10}$$

where the $rp \times n$ matrix P and the $ms \times n$ matrix Q are isometric matrices (all of the columns are orthonormal), leaving the singular values of $H_{rs}(0)$ in the diagonal matrix D with positive elements $[d_1, d_2, \ldots, d_n]$. The rank n of $H_{rs}(0)$ is determined by testing the singular values for zero (relative to desired accuracy)[11] which will be described in the next section. Define

$$H_{rs}(0) = PDQ^T = [PD][Q^T] = P_d Q^T \tag{11}$$

Each of the four matrices $[P_d^T, Q^T, W_s, V_r^T]$ has rank and row number n. By Eq. (5) with $k=0$,

$$V_r W_s = H_{rs}(0) = P_d Q^T \tag{12}$$

Multiplying on the left by P_d^T and solving for Q^T yields

$$TW_s = (P_d^T P_d)^{-1} P_d^T V_r W_s = Q^T \tag{13}$$

The matrix T is nonsingular because if

$$U = W_s Q (Q^T Q)^{-1} = W_s Q$$

then $TU = I$ by Eq. (13). Since $TU = I = UT$ for nonsingular T and U, then

$$W_s [Q (P_d^T P_d)^{-1} P_d^T] V_r = I_n \qquad (14)$$

Hence, by Eq. (14),

$$H^\# = [Q][(P_d^T P_d)^{-1} P_d^T] = [Q][D^{-1} P^T] = Q P_d^\# \qquad (15)$$

The dimension of matrices Q and $P_d^\#$ with rank n are $ms \times n$ and $n \times rp$, respectively. Define 0_p as a null matrix of order p, I_p an identity matrix, $E_p^T = [I_p, 0_p, ..., 0_p]$, and $E_m^T = [I_m, 0_m, ..., 0_m]$.

With the aid of Eqs. (5), (6), and (15), a minimum order-realization can be obtained from

$$Y(k+1) = E_p^T H_{rs}(k) E_m = E_p^T V_r A^k W_s E_m$$

$$= E_p^T V_r W_s H^\# V_r A^k W_s H^\# V_r W_s E_m$$

$$= E_p^T H_{rs}(0) Q P_d^\# V_r A^k W_s Q P_d^\# H_{rs}(0) E_m$$

$$= E_p^T H_{rs}(0) Q [P_d^\# H_{rs}(1) Q]^k P_d^\# H_{rs}(0) E_m$$

$$= E_p^T P_d [P_d^\# H_{rs}(1) Q]^k Q^T E_m$$

$$= E_p^T P D^{\frac{1}{2}} [D^{-\frac{1}{2}} P^T H_{rs}(1) Q D^{-\frac{1}{2}}]^k D^{\frac{1}{2}} Q^T E_m \qquad (16)$$

This is the basic formulation of realization for the ERA. The triple $[D^{-\frac{1}{2}} P^T H_{rs}(1) Q D^{-\frac{1}{2}}, D^{\frac{1}{2}} Q^T E_m, E_p^T P D^{\frac{1}{2}}]$ is a minimum realization since the order n of $P_d^\# H_{rs}(1) Q$ equals the dimension of the state vector x. The same solution, in a different form, for the case where $j_i = t_i = i$ ($i = 1, ..., r-1$), can be obtained by a completely different approach as shown in Refs. 3 and 19. The system [Eqs. (1) and (2)] with this realization is written as

$$\bar{x}(k+1) = D^{-\frac{1}{2}} P^T H_{rs}(1) Q D^{-\frac{1}{2}} \bar{x}(k) + D^{\frac{1}{2}} Q^T E_m u \qquad (17)$$

$$y(k) = E^T P D^{\frac{1}{2}} \bar{x}(k) \qquad (18)$$

where

$$x(k) = W_s Q D^{-\frac{1}{2}} \bar{x}(k) \qquad (19)$$

Now, the case can be summarized as follows.

A finite dimensional, discrete-time, linear time-invariant dynamical system with multi-input and multi-output is realizable in terms of the measurement functions if the system is controllable and observable (the ranks of matrices V_r and W_s are n). A simple exercise, such as replacing $Y(k+1)$ by $Y(k)$ in Eq. (16), shows that the algorithm developed above is also true for the realization of a system with initial state response.

Note that no restrictions on system eigenvalues are given for this case. In other words, this technique can realize a system with repeated eigenvalues. As byproducts of this approach, two alternative algorithms identified as (A1) and (A2) are derived in the Appendix.

Modal Parameter Identification
and Model Reduction

The presence of almost unavoidable noise and structural nonlinearity introduces uncertainty about the rank of the generalized Hankel matrix and, hence, about the dimension of the resulting realization. By employing the singular-value decomposition (SVD) technique, the rank structure of the

Hankel matrix can be displayed quantitatively. The set of singular values can be used to judge the distance of the matrix with determined order to a lower-order one. Therefore, the structure of the generalized Hankel matrix can be properly exploited to solve the realization problem efficiently. These include an excellent numerical performance, stability of the realization, and flexibility in determining order-error tradeoff.

Assume that, by Eq. (10),

$$D = \text{diag}[d_1, d_2, ..., d_n, d_{n+1}, ..., d_N] \qquad (20)$$

with

$$d_1 \geq d_2 \geq ... \geq d_n \geq d_{n+1} \geq ... \geq d_N \qquad (21)$$

If the matrix $H_{rs}(0)$ has rank n then all of the singular values $d_i (i = n+1, ..., N)$ should be zero. When singular values $d_i (i = n+1, ..., N)$ are not exactly zero but very small, then one can easily recognize that the matrix $H_{rs}(0)$ is not far away from an n-rank matrix. However, there can be real difficulties in determining a gap between the computed last nonzero singular value and what effectively should be considered zero, when measurement noise is present. Possible sources of the noise can be attributed to the measurement signal, computer roundoff, and instrument imperfections.

Look at the singular value d_n of the matrix $H_{rs}(0)$. Choose a number δ based on measurement errors incurred in estimating the elements of $H_{rs}(0)$ and/or roundoff errors incurred in a previous computation to obtain them. If δ is chosen as a "zero threshold" such that $\delta < d_n$, then the matrix $H_{rs}(0)$ is considered to have rank n. Unless information about the certainty of the measurement data is given, the number δ is defined as a function of the precision limit in the computer. For example, $\delta = d_n/d_1$ cannot exceed the precision limit; further details are found in Ref. 11.

After the test of singular values, assume that the matrix $[D^{-\frac{1}{2}} P^T H_{rs}(k) Q D^{-\frac{1}{2}}]$ has rank n. Find the eigenvalues z and eigenvectors ψ such that

$$\psi^{-1} [D^{-\frac{1}{2}} P^T H_{rs}(k) Q D^{-\frac{1}{2}}] \psi = z \qquad (22)$$

The modal damping rates and damped natural frequencies are simply the real and imaginary parts of the eigenvalues, after transformation from the z to the s plane using the relationship

$$s = [(\ln z) \pm i2j\pi]/(k\Delta\tau); \qquad i = \sqrt{-1} \qquad (23)$$

where $\Delta\tau$ is the data sampling interval and j is an integer. The integer k is generally chosen as 1 for simplicity. Although z and ψ are complex numbers, computations of Eq. (22) can be performed using a real algorithm[20] since the state matrix realized for flexible structures has independent eigenvectors.

The triple $[z, \psi^{-1} D^{\frac{1}{2}} Q^T E_m, E_p^T P D^{\frac{1}{2}} \psi]$ is obviously a minimum order realization simply by observing Eq. (16). The matrix $E_p^T P D^{\frac{1}{2}} \psi$ is called mode shapes and the matrix $\psi^{-1} D^{\frac{1}{2}} Q^T E_m$ initial modal amplitudes. To quantify the system and noise modes, two indicators are developed as follows.

Modal Amplitude Coherence γ

If the information about the uncertainties of the measurement is minimum, the rank thus determined by the SVD becomes larger than the number of excited and observed system modes to represent the presence of noises in modal space. In modal parameter identification, the indicator referred to as modal amplitude coherence is developed to quantitatively distinguish the system and noise modes. Based on the accuracy parameter, the degree of modal excitation (controllability) is estimated.

The modal amplitude coherence is defined as the coherence between each modal amplitude history and an ideal one

formed by extrapolating the initial value of the history to latter points using the identified eigenvalue. Let the control input matrix (initial condition) be expressed as

$$\psi^{-1} D^{\frac{1}{2}} Q^T E_m = [b_1, b_2, \ldots, b_n]^* \qquad (24)$$

where the asterisk means transpose complex conjugate, and the $1 \times m$ column vector b_j corresponds to the system eigenvalue s_j $(j = 1, \ldots, n)$. Consider the sequence

$$q_j^* = [b_j^*, \exp(t_1 \Delta \tau s_j) b_j^*, \ldots, \exp(t_{s-1} \Delta \tau s_j) b_j^*] \qquad (25)$$

which represents the ideal modal amplitude in the complex domain containing information of the magnitude and phase angle with time step $\Delta \tau$. Now, define vector q_j such that

$$\psi^{-1} D^{\frac{1}{2}} Q^T = [q_1, q_2, \ldots, q_n]^* \qquad (26)$$

The complex vector q_j represents the modal amplitude time history from the real measurement data obtained by the decomposition of the Hankel matrix. Let γ_j be defined as the coherence parameter for the jth mode, satisfying the relation

$$\gamma_j = |\bar{q}_j^* q_j| / (|\bar{q}_j^* \bar{q}_j| \, |q_j^* q_j|)^{\frac{1}{2}} \qquad (27)$$

where $| \ |$ represent the absolute value. The parameter γ_j can have only the values between 0 and 1. $\gamma_j \rightarrow 1$ as $\bar{q}_j \rightarrow q_j$ indicates that the realized system eigenvalue s_j and the initial modal amplitude b_j are very close to the true values for the jth mode of the system. On the other hand, if γ_j is far away from the value 1, the jth mode is a noise mode. However, to make a clear distinction between the system and noise modes requires further study. Obviously, the parameter γ_j quantifies the degree to which the modes were excited by a specific input, i.e., the degree of controllability.

Modal Phase Collinearity μ

For lightly damped structures, normal mode behavior should be observed. An indicator referred to as the modal phase collinearity is developed to measure the strength of the linear functional relationship between the real and imaginary parts of the mode shape for each mode. Based on the accuracy indicator, the degree of modal observation is estimated. Define

$$E_p^T P D^{\frac{1}{2}} \psi = [c_1, c_2, \ldots, c_n] \qquad (28)$$

where c_j $(j = 1, 2, \ldots, n)$ is the mode shape corresponding to the jth realized mode. Let the column vector 1 of order p be

$$1^T = [1, 1, \ldots, 1] \qquad (29)$$

in which p is the number of sensors. Now compute the following quantities for the jth mode shape.

$$\bar{c}_j = c_j^T 1 / p \qquad (30)$$

$$c_{rr} = [\text{Re}(c_j - \bar{c}_j 1)]^T [\text{Re}(c_j - \bar{c}_j 1)] \qquad (31)$$

$$c_{ri} = [\text{Re}(c_j - \bar{c}_j 1)]^T [\text{Im}(c_j - \bar{c}_j 1)] \qquad (32)$$

$$c_{ii} = [\text{Im}(c_j - \bar{c}_j 1)]^T [\text{Im}(c_j - \bar{c}_j 1)] \qquad (33)$$

$$e = (c_{ii} - c_{rr}) / 2c_{ri} \qquad (34)$$

$$\theta = \arctan[e + \text{sgn}(e)(1 + e^2)^{\frac{1}{2}}] \qquad (35)$$

where Re( ) and Im( ), respectively, are the real and imaginary parts of the complex vector ( ), and sgn( ) is the sign of the scalar ( ). The modal phase collinearity μ_j for the jth mode

is then defined as[21]

$$\mu_j = \{c_{rr} + c_{ri}[2(e^2 + 1)\sin^2(\theta) - 1]/e\}/(c_{rr} + c_{ii})$$

$$j = 1, 2, \ldots, n \qquad (36)$$

This indicator checks the deviation from 0-180 degree behavior for components of the jth identified mode shape. The parameter μ_j can have only the values between 0 and 1. $\mu_j \rightarrow 1$ indicates that accuracy of the mode shape is high. On the other hand, if μ_j is away from 1, the jth mode is either a noise mode or the mode is significantly complex.

Model Reduction

The dynamical system is composed of an interconnection of all of the ERA-identified modes. The accuracy indicators allow one to determine the degree of individual mode participation. Model reduction then can be made by truncating all of the modes with low accuracy indicators. The accuracy of the complete modal decomposition process can be examined by comparing a reconstruction of $Y(k)$ formed by Eq. (16) with the original free decay responses, using the reduced model.

Summary of ERA

The computational steps are summarized as follows:

1) Construct a block-Hankel matrix $H_{rs}(0)$ by arranging the measurement data into the blocks with given r, s, t_i ($i = 1, 2, \ldots, s - 1$) and j_i ($i = 1, 2, \ldots, r - 1$), [Eq. (4)].

2) Decompose $H_{rs}(0)$ using singular-value decomposition [Eq. (10)].

3) Determine the order of the system by examining the singular values of the Hankel matrix $H_{rs}(0)$ [Eq. (20)].

4) Construct a minimum-order realization (A, B, C) using a shifted block-Hankel matrix [Eq. (16)].

5) Find the eigensolution of the realized state matrix [Eq. (22)] and compute the modal damping rates and frequencies [Eq. (23)].

6) Calculate the coherence parameter [Eq. (27)] and the collinearity parameter [Eq. (36)] to quantify the system and noise modes.

7) Determine the reduced system model based on the accuracy indicators, reconstruct function $Y(k)$ [Eq. (16)], and compare with the measurement data.

Note that the optimum determination of r, s, t_i and j_i in step 1 above requires further development. This determination is related to the choice of the measurement data to minimize the size of the Hankel matrix $H_{rs}(0)$ with the rank unchanged.
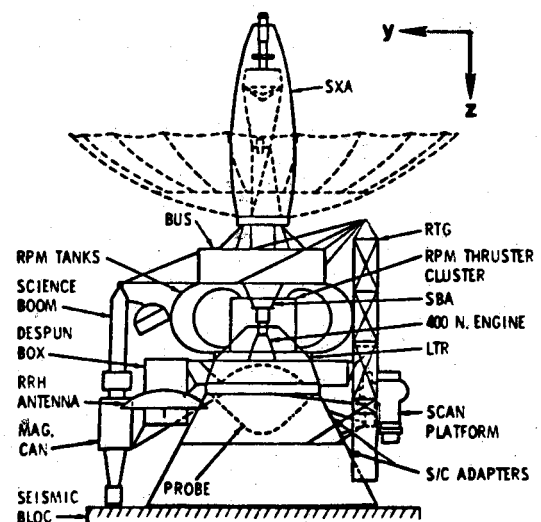

Fig. 1 Galileo spacecraft in launch configuration.

Example: Analysis of Galileo Test Data

The ERA method has been verified using multi-input and multi-output simulation data with or without noise for assumed structures with distinct and/or repeated eigenvalues. The reader is directed to the original version of this paper[22] for more information. Experimental results for the analysis of Galileo test data are given in the following.

The Galileo spacecraft is shown in Fig. 1. All appendages, including the S-X-band antenna (SXA) at the top of the vehicle, were locked in their stowed positions. The structure was cantilevered from its base by bolting the bottom edge of the conical spacecraft adapter ring to a massive seismic block. The adapter ring is the interface between Galileo and a Centaur upper stage that will provide the interplanetary boost.

For dynamic excitation, several electrodynamic shakers of about 100 N capacity, hung on soft suspensions from overhead cranes, were attached at various points. Response measurements were made with 162 accelerometers distributed over the test article.

The finite element model of the structure in this configuration predicted 45 modes of vibration below 50 Hz, with the lowest frequency at about 13 Hz. However, as discussed in Ref. 23, many of the modes are of lesser importance based on their predicted contribution to the dynamic launch loads. In fact, only about 15 modes are major contributors. The presence of the others, however, interspersed in frequency with the important ones, results in high modal density and makes accurate parameter identification more difficult.

Complete details of the test configuration, analytical model predictions, and the method used to estimate the relative importance of the modes, can be found in Ref. 23.

Test and Data Acquisition Procedures

All results to be presented were obtained from two sets of free-response measurements recorded following single-point random excitation of the structure. The first data set was obtained using single-shaker, lateral excitation—in the global x direction—and the second set with single shaker, vertical excitation—in the global z direction. These tests are referred to as simply the "x direction" and "z direction" tests. For both tests, no special effort was made to select the position for the shaker. Each position was chosen using only the knowledge that many modes were excited from the location in previous tests. Other than the point and direction of excitation, all

characteristics of the test, data acquisition, and data-reduction processes were exactly the same for both data sets.

The random excitation signal, bandlimited to the interval from 10 to 45 Hz, was generated digitally with the same test system which was also used to record the accelerometer response signals. Approximately 5 s of data were recorded following the end of the excitation signal. The responses were digitized at a rate of 102.4 samples per second, resulting in about 500 free-response points in each test.

Identified Eigenvalues

Each ERA analysis was performed using a single matrix of data from all 162 response measurements and one initial condition (either x- or z-direction test) at a time. Each response function Y as shown in Eq. (4) was thus a 162×1 matrix. Using $j_1 = 1$ and $t_i = i$ ($i = 1,2,...,499$) the Hankel matrix H_{rs} of 324 rows by 500 columns was formed to perform the analysis.

A summary of the identification results for the x direction test is provided in Table 1, including identified frequencies, damping factors, and accuracy indicators. The results for the z-direction test can be found in Ref. 24. These results closely agree with those obtained by other experimental techniques as shown in Refs. 17 and 25.

Table 1 ERA-identified results for x-direction

Mode No.	Frequency, Hz	Damping factor, %	Accuracy indicators γ[a]	μ[b]	Max.[c]	No.[d]
1	13.613[e]	3.301	98.6[e]	99.0	0.104	6
2	14.153[e]	1.645	99.8[e]	94.2	0.063	5
3	18.369[e]	1.409	99.7[e]	98.7	0.270	59
4	18.680[e]	1.086	99.7[e]	79.8	0.068	17
5	19.516[e]	0.659	96.5[e]	99.1	0.090	23
6	22.040	8.311	50.7	43.1	0.009	0
7	22.047[e]	0.777	98.9[e]	97.7	0.122	58
8	22.132[e]	0.356	97.5[e]	99.3	0.088	45
9	22.640[f]	1.282	93.1[f]	86.6	0.018	4
10	25.126[e]	1.515	99.8[e]	89.8	0.239	27
11	25.751[g]	5.569	80.2[g]	56.2	0.043	15
12	25.871[e]	0.806	98.6[e]	99.4	0.279	67
13	28.517[e]	0.835	97.7[e]	98.0	0.121	10
14	29.659[f]	1.723	91.7[f]	61.2	0.010	1
15	30.940[e]	3.003	98.2[e]	77.1	0.059	5
16	32.828	6.668	67.9	52.8	0.015	2
17	33.288[f]	2.894	93.4[f]	44.0	0.012	4
18	33.613[e]	1.326	98.1[e]	59.8	0.024	3
19	34.402[e]	1.057	98.2[e]	98.4	0.047	15
20	36.890[f]	1.633	93.3[f]	73.1	0.020	2
21	37.631	5.957	50.0	76.2	0.041	2
22	38.019[f]	0.575	94.1[f]	44.9	0.008	0
23	39.551	4.048	75.5	99.2	0.240	5
24	41.021[f]	2.038	92.4[f]	89.8	0.123	17
25	42.169	3.737	65.2	89.1	0.022	6
26	42.273[f]	1.124	92.9[f]	68.5	0.011	3
27	43.758[f]	1.614	94.2[f]	57.7	0.019	3
28	44.892[e]	0.394	99.4[e]	99.1	0.513	24
29	45.173	4.188	79.6	67.0	0.021	6
30	45.174	0.835	78.5	78.7	0.041	3
31	47.191[g]	2.126	84.3[g]	50.8	0.008	0
32	48.311[f]	1.214	94.4[f]	78.3	0.034	5
33	48.414	3.300	59.2	57.0	0.014	3
34	50.385[g]	1.143	89.5	40.2	0.027	3

[a] γ%: Modal amplitude coherence.
[b] μ%: Modal phase collinearity.
[c] Maximum modal participation in g's among the 162 components identified. (The measurement noise floor was approximately 0.002 g.)
[d] Number of mode shape components of 162 with initial response amplitude > 0.01 g. Indicator of local or global response.
[e] $95\% \leq \gamma \leq 100\%$.
[f] $90\% \leq \gamma < 95\%$.
[g] $80\% \leq \gamma < 90\%$.

Frequency = 13.613 Hz   Damping = 3.301%
Modal Amplitude Coherence = 98.6%   Modal Phase Colinearity = 99.0%

(a) 13.613 Hz antenna bending mode from x-direction random test.

Frequency = 38.037 Hz   Damping = .513%
Modal Amplitude Coherence = 99.8%   Modal Phase Colinearity = 93.1%

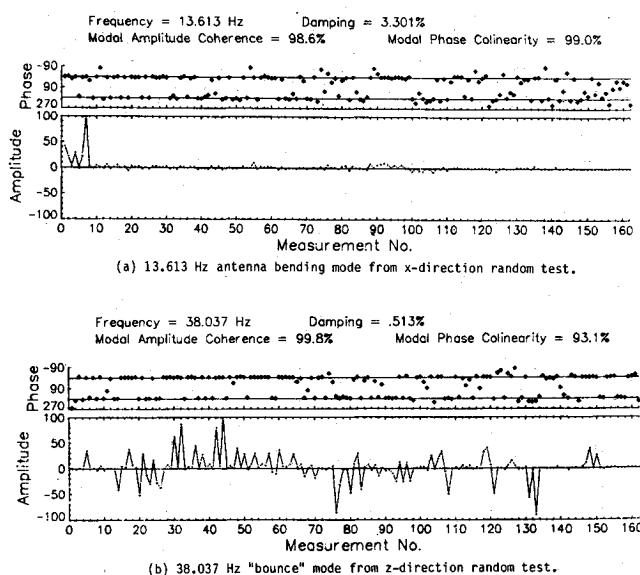(b) 38.037 Hz "bounce" mode from z-direction random test.

Fig. 2 Example ERA-identified mode shapes illustrating various degrees of phase angle scatter.

The best single accuracy indicator now available is the modal amplitude coherence. Its value is used in Table 1 to rate the identified modes at various degrees of accuracy. The rating scale is noted in the key beneath the table. A brief description of the information in each of the three columns on the far right of the table is also contained in the keys. The significance of modal phase collinearity will be discussed in the next subsection. The data in the last two columns are two additional indications of the strength of the modal response signals relative to the instrumentation noise floor. These indicators are computed using modal participation values in physical units, which are the products of the mode shapes and the initial modal amplitudes.

Identified Mode Shapes

Two typical ERA-identified mode shapes are shown in Fig. 2. Based on these results and observations from other data not shown, the following conclusions can be drawn.

1) The local behavior of many of the Galileo modes—exemplified by the antenna mode shown in Fig. 2a in which only about five measurements show motion—makes it more difficult to identify all 162 components of the mode shapes accurately because of the low response levels.

2) A good measure of the effects of noise on the mode shape accuracy is often indicated by the amount of scatter in the identified modal phase angles from the ideal 0-180 deg normal mode behavior. Of course, true complex-mode behavior needs to be differentiated from identification scatter due to noise and nonlinearity. The best remedy is to compare the results for the same mode obtained in several different tests.

3) The parameter referred to as the modal phase collinearity can be used to measure how closely the modal phase angle results for each mode cluster near 0 and 180 deg. Calculated using principal component analysis, it indicates the extent to which the information in each complex-valued mode shape is representable as a real-valued vector. It ranges from a value of zero for no collinearity to 100% for perfect collinearity.

4) Based on studies with simulated data, the accuracy of mode shapes showing clustering of the identified phase angles near 0 and 180 deg, such as in Fig. 2, can generally be accepted with little questioning. However, those modes with significantly more phase angle scatter should not be used without further confirmation.

5) Most mode-shape components whose identified phase angles are displaced from the 0- and 180-deg lines are those with the smallest amplitudes. This characteristic is consistently observed in the result shown in Fig. 2b. Small modal amplitude results for these components, however, usually indicate accurately that the response amplitude is, in fact, very small. This information is all that can be expected from a measurement standpoint, and is all that is required in many instances.

Identified Modal Amplitudes

The ERA modal amplitude coherence indicates the purity of the individual modal amplitude time histories. For each identified eigenvalue, a modal amplitude time sequence is obtained for each initial condition. These data provide a direct indication of the strength with which the mode was identified in the analysis. For strongly identified modes, the modal amplitude history is a pure, exponentially decaying sinusoid of the corresponding frequency and damping, which decays smoothly over the entire analysis interval. For weakly identified modes, the modal amplitude history is distorted. In particular, the history is a sequence of noise for any eigenvalue not corresponding to a structural mode.

Typical examples of modal amplitude results from the Galileo analysis are shown in Fig. 3. These data were selected to illustrate the variation in the purity of the modal amplitude histories for a mode which was strongly excited is only one of the two ERA tests.

The mode shown in Fig. 3, at approximately 38 Hz, is the fundamental z-direction "bounce mode" of the structure. As would be expected, the modal amplitude plots confirm that the mode was more strongly excited in the z-direction test than in the x-direction test. This conclusion is reflected in the modal amplitude coherence shown in Fig. 3a compared with that in Fig. 3b.

Data Reconstruction

The final aspect of the ERA method available for assessing identification accuracy is the process of data reconstruction. This procedure consists of comparing the original free-response time histories (and their frequency spectra) with those calculated using the ERA-reduced model, which contains 22 modes with high modal amplitude coherence. If the ERA modal decomposition process is performed accurately, the reconstruction results will closely match the original data.

Figure 4 shows a typical such comparison from the Galileo data analysis. The two time histories are compared at the top of the figure, and their fast Fourier transforms (FFT), in both amplitude and phase, in the lower plots. The reconstruction result, the smoother of the two lines in the FFT plots, is seen to closely follow the original data in both amplitude and phase. The increase in amplitude of the test data below 2 Hz is due to residual motion of the shaker on its soft suspension. These response characteristics, well below the first flexural
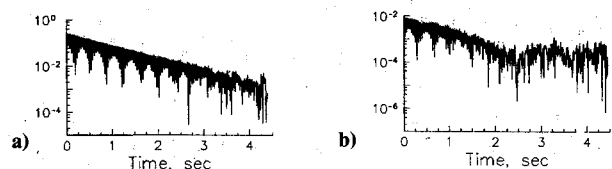

Fig. 3 Example modal amplitude results. This mode near 38 Hz is the fundamental z-direction "bounce mode" of the structure. Comparison of a and b shows that the mode was more strongly excited in the z-direction test, as expected. a) 38.037-Hz modal amplitude from z-direction test; modal amplitude coherence = 99.8%. b) 38.019-Hz modal amplitude from x-direction test; modal amplitude coherence = 94.1%.
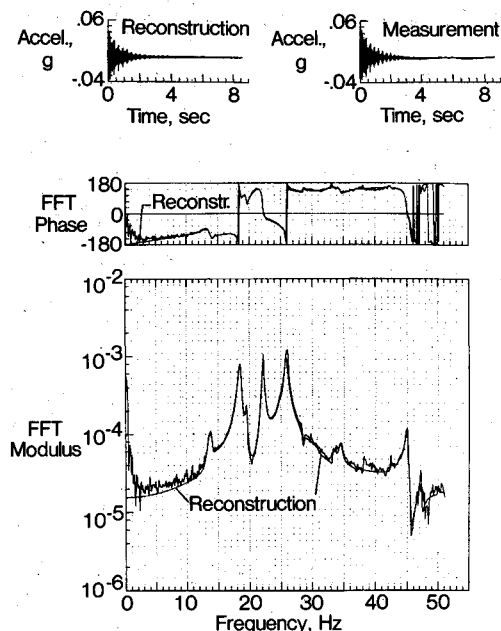

Fig. 4 Example comparison of a measurement from x-direction test with a 22-mode reconstruction.

mode of the spacecraft, do not affect the modal results and were not retained in the identified parameter set.

Concluding Remarks

An eigensystem realization algorithm is developed for modal parameter identification and model reduction for dynamical systems. Two developments are given in this paper. First, a new approach is developed to derive the basic formulation of minimum realization for dynamical systems. As byproducts of this approach, two alternative less powerful algorithms, identified as algorithms (A1) and (A2), are derived. A special case of (A1) is shown to be equivalent to an approach currently in use in the structural dynamics field. Second, accuracy indicators are developed to quantify the participation of system modes and noise modes in the realized system model. In other words, the degree of controllability and observability for each participating mode is determined. A model reduction then can be made for controller design.

Based on the results of other analyses of simulated data, the parameters referred to as modal amplitude coherence and modal phase collinearity are good indicators of the identification accuracy that is achieved. Using these indicators, approximately 15 modes from the Galileo analysis are judged to be of high accuracy. Less than 10 min of CPU time on a CDC mainframe computer were required for the Galileo analysis. However, additional research is needed to correctly assess the degree of accuracy achieved by those modes showing significant identification scatter. The effects of structural nonlinearities on the results also need further attention.

Important features of the eigensystem realization algorithm are summarized as follows.

1) From the computational standpoint, the algorithm is attractive since only simple numerical operations are needed.

2) The computational procedure is numerically stable.

3) The structural dynamics requirements for modal parameter identification and the control design requirements for a reduced state space model are satisfied.

4) Data from more than one test can be used simultaneously to efficiently identify closely spaced eigenvalues.

5) Computation requirements are moderate.

Appendix

In view of Eqs. (4) through (6), the measurement function $Y(k+1)$ can be obtained through either of two other algorithms [Eqs. (A1) and (A2)]. The algorithm (A1) is

$$Y(k+1) = E_p^T H_{rs}(k) E_m = E_p^T V_r A^k W_s H^\# V_r W_s E_m$$

$$= E_p^T [V_r A W_s H^\#]^k V_r W_s E_m$$

$$= E_p^T [H_{rs}(1)H^\#]^k H_{rs}(0) E_m \qquad (A1)$$

and the algorithm (A2) is

$$Y(k+1) = E_p^T H_{rs}(k) E_m = E_p^T V_r W_s H^\# V_r A^k W_s E_m$$

$$= E_p^T V_r W_s [H^\# V_r A W_s]^k E_m$$

$$= E_p^T H_{rs}(0) [H^\# H_{rs}(1)]^k E_m \qquad (A2)$$

Hence, by Eq. (3), $[H_{rs}(1)H^\#, H_{rs}(0)E_m, E_p^T]$ or $[H^\# H_{rs}(1), E_m, E_p^T H_{rs}(0)]$ is a realization. The system [Eqs. (1) and (2)] with realization (A1) will be transformed into the following equation:

$$\bar{x}(k+1) = H_{rs}(1)H^\#\bar{x}(k) + H_{rs}(0)E_m u$$

$$y(k) = E_p^T \bar{x}(k)$$

where $x(k) = V_r H^\#\bar{x}(k)$. Or, using Eq. (A2),

$$\bar{x}(k+1) = H^\# H_{rs}(1)\bar{x}(k) + E_m u$$

$$y(k) = E_p^T H_{rs}(0)\bar{x}(k)$$

where $\bar{x}(k) = W_s x(k)$.

These realizations are not of minimum order, since the dimension of x is the number of either columns or rows of the matrix $H_{rs}(0)$ which is larger than the order n of the state matrix A for multi-input and multi-output cases. Examination of Eqs. (A1), (A2), and (16) reveals that algorithms (A1) and (A2) are special cases of ERA. Algorithm (A1) is formulated by inserting the identity matrix (6) on the right-hand side of the state matrix A as shown in Eq. (A1). On the other hand, algorithm (A2) is obtained by inserting the identity matrix (6) on the left-hand side of the state matrix A as shown in Eq. (A2). However, ERA is formed by inserting the identity matrix (6) on both sides of the state matrix A as shown in Eq. (16). Because of the different insertion, algorithms (A1) and (A2) do not minimize the order of the state transition matrix. Mathematically, if the singular-value decomposition technique is not included in the computational procedures [see Eqs. (8) and (9)], Eqs. (A1) and (A2) cannot be numerically implemented, unless a certain degree of artificial noise and/or system noise are present. Noises tend to make up the rank deficiency of the generalized Hankel matrix $H_{rs}(0)$ for algorithms (A1) and (A2). Since the degree of noise contamination is generally unknown, algorithms (A1) and (A2) are not recommended.

References

[1]Gilbert, E.G., "Controllability and Observability in Multivariable Control Systems," *SIAM Journal on Control*, Vol. 1, No, 2, 1963, pp. 128-151.

[2]Kalman, R.E., "Mathematical Description of Linear Dynamical Systems," *SIAM Journal on Control*, Vol. 1, No. 2, 1963, pp. 152-192.

[3]Ho, B.L., Kalman, R.E., "Effective Construction of Linear State-Variable Models from Input/Output Data," *Proceedings of the 3rd Annual Allerton Conference on Circuit and System Theory*, 1965, pp. 449-459; also, *Regelungstechnik*, Vol. 14, 1966, pp. 545-548.

[4]Tether, A.J., "Construction of Minimal Linear State-Variable Models from Finite Input-Output Data," *IEEE Transactions on Automatic Control*, Vol. AC-15, No. 4, Aug. 1970, pp. 427-436.

[5]Silverman, L.M., "Realization of Linear Dynamical Systems," *IEEE Transactions on Automatic Control*, Vol. AC-16, No. 6, 1971, pp. 554-567.

[6]Rossen, R.H., and Lapidus, L., "Minimum Realizations and System Modeling: I. Fundamental Theory and Algorithms," *AIChE Journal*, Vol. 18, No. 4, July 1972, pp. 673-684.

[7]Rossen, R.H.. and Lapidus, L., "Minimum Realizations and System Modeling: II. Theoretical and Numerical Extensions," *AIChE Journal*, Vol. 18, No. 5, Sept. 1972, pp. 881-892.

[8]Zeiger, H.P. and McEwen, A.J., "Approximate Linear Realizations of Given Dimension Via Ho's Algorithm," *IEEE Transactions on Automatic Control*, Vol. AC-19, No. 2, April 1974, pp. 153.

[9]Kung, S., "A New Identification and Model Reduction Algorithm Via Singular Value Decomposition," *12th Asilomar Conference on Circuits, Systems and Computers*, Nov. 1978, pp. 705-714.

[10]Golub, G.H. and Reinsch, C., "Singular Value Decomposition and Least Squares Solutions," *Numerical Mathematics*, Vol. 14, 1970, pp. 403-420.

[11]Klema, V.C. and Laub, A.J., "The Singular Value Decomposition: Its Computation and Some Applications," *IEEE Transactions on Automatic Control*, Vol. AC-25, No. 2, April 1980, pp. 164-176.

[12]Stroud, R.C., Smith, S., and Hamma, G.A., "MODALAB—A New System for Structural Dynamic Testing," *Shock and Vibration Bulletin*, No. 46, Pt. 5, Aug. 1976, pp. 153-175.

[13]Ibrahim, S.R. and Mikulcik, E.C., "A Method for the Direct Identification of Vibration Parameters from the Free Response," *Shock and Vibration Bulletin*, No. 47, Pt. 4, Sept. 1977, pp. 183-198.

[14]Brown, D.L., Allemang, R.J., Zimmerman, R. and Mergeay, M., "Parameter Estimation Techniques for Modal Analysis," *SAE Paper 790221*, Feb. 1979.

[15]Coppolino, R.N., "A Simultaneous Frequency Domain Technique for Estimation of Modal Parameters from Measured Data," SAE Paper 811046, Oct. 1981.

[16]Vold, H. and Russell, R., "Advanced Analysis Methods Improve Modal Test Results," Sound and Vibration, March 1983, pp. 36-40.

[17]Chen, J.C., "Evaluation of Modal Testing Methods," AIAA Paper 84-1071, May 1984.

[18]Chen, C.T., Introduction to Linear System Theory, Holt, Rienhart, and Winston, Inc., New York, 1970.

[19]Kalman, R.E., and Englar, T.S., "Computation of a Minimal Realization," A User Manual for the Automatic Synthesis Program, NASA CR-475, June 1966, Chap XV.

[20]Gantmacher, F.R., The Theory of Matrices, Vol. 1, Chelsea Publishing Co., New York, New York, 1959.

[21]Moore, B.C., "Principal Component Analysis in Linear Systems: Controllability, Observability, and Model Reduction," IEEE Transactions on Automatic Control, Vol. AC-26, No. 1, Feb. 1981, pp. 17-32.

[22]Juang, J.N. and Pappa, R.S., "An Eigensystem Realization Algorithm (ERA) for Modal Parameter Identification and Model Reduction," NASA/JPL Workshop on Identification and Control of Flexible Space Structures, San Diego, Calif., June 1984.

[23]Chen, J.C. and Trubert, M., "Galileo Modal Test and Pre-Test Analysis," Proceedings of the 2nd International Modal Analysis Conference, Orlando, Fla., Feb. 1984, pp. 796-802.

[24]Pappa, R.S. and Juang, J.N., "Galileo Spacecraft Modal Identification Using an Eigensystem Realization Algorithm," The Journal of the Astronautical Sciences, Vol. 33, No. 1, Jan.-March, 1985, pp. 15-33.

[25]Stroud, R.C., "The Modal Survey of the Galileo Spacecraft," Sound and Vibration, April 1984, pp. 28-34.